Available online at www.sciencedirect.com

jmr&t Journal of Materials Research and Technology

journal homepage: www.elsevier.com/locate/jmrt

Original Article

Quantitative analysis of the effects of incorporating laser powder bed fusion manufactured conformal cooling inserts in steel moulds over four types of defects of a commercially produced injected part

Joaquim Minguella-Canela [a,*], *Sergio Morales Planas* [b], *Vicente César de Medina Iglesias* [c], *M. Antonia de los Santos López* [c]

[a] *Grup de Recerca en Tecnologies de Fabricació (TECNOFAB), Departament D'Enginyeria Mecànica (DEM), Escola Tècnica Superior D'Enginyeria Industrial de Barcelona (ETSEIB), Universitat Politècnica de Catalunya (UPC), Campus Sud, Edif. PF, Av. Diagonal 647, 08028, Barcelona, Spain*

[b] *Fluidra S.A., Av. Alcalde Barnils, Nº 69, 08174, Sant Cugat Del Vallès, Barcelona, Spain*

[c] *Centre de Recerca de Motors I Instal·lacions Tèrmiques (CREMIT), Departament de Màquines I Motors Tèrmics (MMT), Escola Tècnica Superior D'Enginyeria Industrial de Barcelona (ETSEIB), Universitat Politècnica de Catalunya (UPC), Campus Sud, Edif. PF, Av. Diagonal 647, 08028, Barcelona, Spain*

ARTICLE INFO

Article history:
Received 9 November 2022
Accepted 21 February 2023
Available online 26 February 2023

Keywords:
Laser powder bed fusion
Steel
ooling inserts
Conformal cooling
Moulds additive manufacturing

ABSTRACT

The introduction of additively manufactured conformal cooling inserts in steel moulds for plastic injection is becoming a recommended standard. Fine adjustment of the temperatures in the mould has demonstrated potential to reduce cycle times and to increase production volumes. Within this context, the present article explores the historical production data of a commercially produced part, before and after the incorporation of an L-PBF conformal cooling insert, to analyse what is the quantitative real effect on the efficiency of the production runs. The article analyses the change in the global rejection rates, and its effect over four different product defect types, i.e.: optical (surface), part integrity (bubbles, transparency, geometry), incomplete fill-in (interior), and breakages during extraction. The results demonstrate a specific decrease on the average appearance (from 20.53% to 13.48%; reduction of 7.05%) and variability (standard deviation from 14.16% to 6.81%; reduction of a 7.35%), of the global scrap rates, and a significant decrease in the scrap rates generated by optical defects and extraction part breakages. The article also characterises the former and the new processes by adjusting two distribution functions (Pareto Type-I and Weibull) and compares different estimates for the global expected scrap rates in past and future production runs.

* Corresponding author.
E-mail address: joaquim.minguella@upc.edu (J. Minguella-Canela).

https://doi.org/10.1016/j.jmrt.2023.02.164

1. Introduction

Injection moulding operations have a large share of processing time dedicated to the cooling of the injected material. In the general case for plastic parts, this share remains being up from 50% to 70% of the total processing time [1]. The introduction of conformal cooling channels (CCC) in steel moulds for plastic injection has been prescribed during the last years as a most advised standard for improving the moulds capabilities, thus boosting the production capacities, and achieving moulded products that were impossible to obtain beforehand [2]. And the introduction of additive manufacturing and associated technologies to obtain such CCC in mould inserts has shown to be an excellent manner to unleash the attainment of such moulding new capabilities [3–8].

To this respect, it is feasible to obtain CCC with many different AM processes, either with direct or indirect fabrication [9]. For instance, polymer AM has been presented as a procedure capable to produce soft inserts for injection moulding [10] and have claimed energy and time consumption during production to be significantly lower. However, as polymeric inserts lifetime is significantly shorter than that of metallic inserts; multiple inserts are generally needed to meet a specific production batch size [11,12].

Apart from these examples, the use of Laser Powder Bed Fusion (L-PBF) AM, such as Selective Laser Melting (SLM), in which metallic powder is laser-processed layer-by-layer, is one of the most significant procedures to obtain almost fully dense metal inserts [13–17]. Indeed, hybrid L-PBF (combining laser AM and subtractive processes) is regarded as the future direction of manufacturing for obtaining high dimensional-accuracy moulds incorporating CCC, although there is still a large potential to reduce costs and to raise efficiency [18].

In this context, most of the characterisation efforts for the results of such paradigm change have been discussed at a prior evaluation level [19], at a prototype level (conveying simulation and/or physical demonstration) [20–23], at a case study level [24,25], and even at a production set-up level [26]. Nevertheless, there is a lack of studies targeting real manufacturing results data series. In this sense, it is pertinent to assess a relatively long historical production data of a commercially produced part, before and after the incorporation of an AM conformal cooling insert, to analyse what is the quantitative real effect on the efficiency of the production runs.

Therefore, the present article analyses the overall rejection rates of a commercial product manufactured via injection moulding, as well as the behaviour of four different product defect types comparing the situation before and after introducing such AM insert containing CCC. The initial hypothesis of the redesign is that global scrap rates will be reduced sustainably over time, as well as the types of defects related to the temperature behaviour of the set. The paper also characterises the former process and the latter process finding an adjustment regarding two distribution functions as a proxy to understand the nature of the changes in the behaviour of the process. Finally, it compares confidence intervals for the global expected scrap rates in future production runs.

1.1. *Utilisation of AM inserts containing CCC*

Utilising AM inserts containing CCC have demonstrated yielding many advantages. The most notorious of them is probably the freedom of design of the geometries, which is of particular interest when addressing complex designs. In particular, the use of SLM enables doing so without compromising the mechanical properties achieved [27–30]. Indeed, such channels can work variable depths, lengths, and widths along the paths, following organic splines near to the surfaces that need to be cooled. Thin walls down to 0.3 mm have been reported to be possible depending on the application [31]. All this, considering that L-PBF cooling channels will have not the same behaviour and capabilities as drilled channels [32], with dimensional accuracy depending heavily on the channel orientation respect to the build direction [33], and with horizontal channels demonstrating the poorest dimensional accuracy due to the lack of supports in the central overhanging regions [34], which lead the top roof of them to have a typically rough profile like fluffy cotton reaching values of surface roughness in the R_a range from 15.4 μm to 26 μm [35]. Indeed, the roughness levels in the interior of the CCC will be crucial to improve the heat transfer efficiency of the mould, which is complex as the metal AM processes yield as-built surfaces that are far from the values considered to meet common industry requirements [36].

To this respect, Metal AM surface roughness optimisation can be tackled via best practices on selecting processing parameters [37–39], or by the tuning of L-PBF processes, for example utilising a dual laser setup [40]. Additionally, some post-processing can be applied for optimizing the surface finishing in the complex internal channels, normally involving abrasive flows and/or of chemical attack. However, even surface texture characterisation of AM components is a challenge, as the nature of their surfaces trials the users in selecting an appropriate parameters of cut-off wavelength (λ_c), evaluation length (l_n), and measurement areas [41]. Also, measuring roughness and waviness throughout CCC is complex to be conveyed non-destructively, as many surfaces can be hard or impossible to reach. Techniques such as X-ray computed tomography (XCT) [42] are key to ensure a suitable level of characterisation and control.

In any case, from the design point of view, the tool-less AM production nature enables quick iterations, and almost every geometry designed is possible to be manufacturable. The use of internal lattice structures makes possible to reduce production times and material use, which in turn reduces costs [7]. As stated previously, it is combinable with traditional manufacturing processes, for example, to obtain hybrid geometries and to incorporate benefits of postprocessing techniques [18,43–46].

Moreover, the refrigeration using such CCC allows a fine adjustment of the temperature distribution in the critical places of the mould operation, yielding cycle times reduction [47,48], and therefore a potential increase in production volumes. Consequently, the overall productivity is expected to be optimised, thus lowering the relative cost per part. In particular, some initial studies of AM tooling inserts yielded figures of reduction in the cycle time up to 15% [49], although more

recently it is being acknowledged that the total reduction can range between 15% and 20% with proper design of the CCC spacing, optimised pipe diameter and the selection of an optimal coolant flow rate [1], or even up to a 35% in certain applications [50], as well as a 24% reduction in cooling time [22].

Finally, concerning durability, several studies also reported that, in metallic moulds incorporating CCC, hardness, tensile strength, and resistance to corrosion over time is extended [51–53], thus extending its useful life [54], and making possible a reduction of the relative contribution to each produce part of the fixed costs associated with the development of the moulds and inserts. However, ductility and fatigue life depend mostly on surface and internal defects, and often found to be poorer [55,56]. In this sense, given the high tooling costs, such developments are specially indicated for long-run production products, capable of finding a breakeven point before reaching the actual intended batch size [57,58].

1.2. *Specification and characteristics of the targeted defect types*

According to the production procedures followed at the company production site of the targeted part of the study (SACOPA-Fluidra group, Barcelona, Spain), the production defects generating scrap are specified into four main different groups of defect types. These four big groups of defect types are the following: (1) defects in the exterior, (2) defects in the interior, (3) integrity, and (4) damages due to the breakages when extracting the produced parts. These types of defects, which are illustrated in Fig. 1, are described in the following subsections, and are very related to the fact that the objective part is transparent and is normally installed in a very visible place.

1.2.1. *Defect type 1: surface defects (spots and superficial finish)*

The first group of type of defects concerns the parts considered flawed due to the existence of superficial imperfections, such as superficial spots, scratches and other deficiencies on the surface that affect the part exterior appearance and shine. These types of defects can be caused by a flow instability (such as plastic moving at different speeds) close to the free surface during the filling stage of the mould [59]. The causes could be linked to insufficient injection speeds and/or injection pressures, which have been recalled conveying anticipated material setting.

Placing the material entrances to the mould in areas in which the material must run the shortest possible displacement is seen as a positive aspect to address this sort of issues. Also, another the suggested response is to increase both mould and material temperatures prior to the fill-in operation. Therefore, as the CCC will locally modify the temperatures in some mould areas, it will be of interest to see if there is any significant change in the occurrence of this defect type.

1.2.2. *Defect type 2: integrity defects (bubbles, transparency, geometry)*

The second group of types of defects includes all parts considered not acceptable due to flaws in the interior of the injected material. This mainly includes bubbles and confined gases in the interior; as well as drawholes, and other aspects such as dyed material that affect the transparency levels of the parts. Sorts of defects such as interior bubbles and/or weld line shrinkage change the density of the sample at their locations. So that, the density distribution (which should be uniform) and the average density of the part are therefore affected by these defects [60]. This sort of defect can be caused by high melt temperatures during the injection, producing gas inside the moulds, as well as insufficient back pressure or oversized decompression. For this reason, it will be of interest to evaluate the impact of the introduction of CCC in terms of if there will be any significant change in the occurrence of this defect type, as the insert will modify the temperatures in some mould areas.

On different terms, it has also been reported that this sort of defects could be caused by the moisture absorbed by the raw material prior to its utilisation [61], although this cause of defect does not relate directly to the injection moulding operation and should be controlled separately prior to the mould processing. Lastly, this category of defect also includes the number of parts that have been reported to be out of geometrical specifications. However, the occurrence of this subset in the initial situation is very reduced -only 32 parts out of the total were reported to have this condition-, letting this to be a marginal occurrence throughout the covered study period.

1.2.3. *Defect type 3: incomplete fill-in*

The third group of types of defects focuses on the parts that are not completely constructed (some material is missing). General process experience describes that this sort of defect can occur if the entrances are not wider enough or if they get blocked. Also, if air pockets are imprisoned during the material injection or if the injection pressure is insufficient. Finally, material viscosity and mould temperature are also defining factors. As most of these parameters can be controlled during the process design stage, the rates for this type of defect have historically accounted for a stable figure. Again, as the CCC will locally modify the temperatures in some mould areas, it will be of interest to see if there is any significant change in the occurrence of this defect type.

1.2.4. *Defect type 4: breakages when extracting the injection parts*

Finally, given the specific part targeted in the present article, there is a fourth defect type that is relevant to be assessed separated than the rest, as in the historical record had a noteworthy appearance. This type of defect is that of parts that suffer a breakage during the extraction from the mould (cracking during part removal), causing the part to be not useable for its envisaged function.

This sort of defect can be caused by the geometry of the part, especially if it contains sharp corners that could accumulate stress, being one of the most appropriate solutions to introduce changes on the part geometry. If the geometry cannot be extensively modified, another possible solution can be to modify the mould temperature distribution, so to avoid the material to be stick to the mould and to degrade after the fill in into a specimen that can be broken during the operator handling.

This type of defect is the one that originated the idea to introduce a CCC to reduce the rates of parts that were to be scrapped.

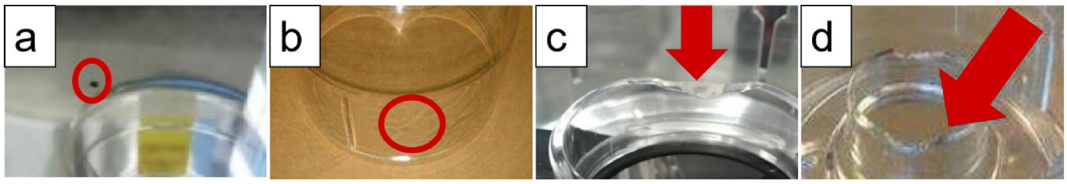

Fig. 1 – Examples of parts with the different types of defects according to the production facility specification: (a) Surface, (b) Integrity, (c) Incomplete fill-in, and (d) Breakage from extraction.

2. Materials and methods

The study focuses on the analysis of the production data accumulated during more than one and a half years of real manufacturing of a single injection moulding part type in a single industrial production site (SACOPA-Fluidra group, Barcelona, Spain). In approximately half of this time the production was performed using with an insert without conformal cooling means (initial period), while the rest of the manufacturing responds to the introduction of a conformal cooling insert in the mould (final period).

In both periods the part geometry and quality requisites stayed invariant, as well as the rest of the utilisation of production means, being the specifically designed conformal cooling insert introduction, the only modification undertaken in the process.

2.1. *Specifications for part and moulds*

The part object of the present study is a plastic funnel utilised in the assemble of a food conduction element. The part is produced in transparent Co-polyester EASTAR (TM) DN011 (Eastman Chemical Company (Kingsport, Tennessee)), and therefore the possible defects are easy to be identified both in its interior and its exterior. Also, this part is assembled in a visible section of the set; thus, the optical appearance of the part is of vital importance for the quality validation. Images of the part to be produced can be found in Fig. 2.

The utilised polymer provides a Tensile Stress of 45 MPa at Yield, and of 44 MPa at Break. With Elongations of 5% at Yield, and 250% at Break. The Flexural Modulus is of 1950 MPa, the Flexural Strength is of 66.5 MPa and the Optical total transmittance of a 90% [62].

To produce the targeted part, the injection moulding operation is undertaken in a KraussMaffei 500Tn injection machine (KraussMaffei Group (Munich, Germany)), with a maximum injection pressure of 184 MPa, and cooled by water at a constant flowrate of 2.5 bar. The mould contains a single cavity, which can be at 15–40 °C following the materials specifications, whist the mould processing melt temperature is to be in the range of 250–270 °C. The drying temperature is of 75 °C and the Mould shrinkage parallel to flow is expected to be of 0.004 mm/mm. The mould is designed for very long series of injection and requires having a high resistance to corrosion to ensure a long-lasting durability. Therefore, following the internal company directives, the material utilised for the cavities is Corrax® (Uddeholm (Hagfors, Sweden)) treated as Aged Steel with a Hardness of 46–48 HRC, and the material utilised for the insert is Stavax 1.2083 ESR (Uddeholm (Hagfors, Sweden)) Hardened to 50–52 HRC.

With these production means (see Fig. 3), and with the initial moulds not incorporating CCC in the insert, the initial injection moulding operation is performed in a total of 105 s, of which 2.8s correspond to the filling in time, 6s to the packing time, and 75s to cooling time.

After the injection moulding part is produced, an assemble with several other components is performed, which normally includes some thin-walled metal parts (laminates) as well as other injection moulded parts (mainly a hat and a cover). The parts are packed in carton boxes and placed in Europallets, forming in each case 4 layers of 13 boxes (total of 52 assembled sets per pallet).

2.2. *Design and integration of the conformal cooling insert*

The design of the insert utilised to obtain the targeted part geometry includes walls which are relatively tall (60 mm

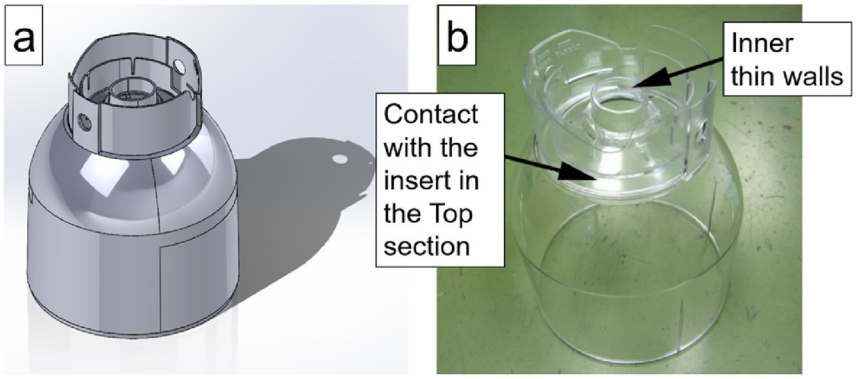

Fig. 2 – Objective part to be produced: (a) 3D model, (b) Injected part.

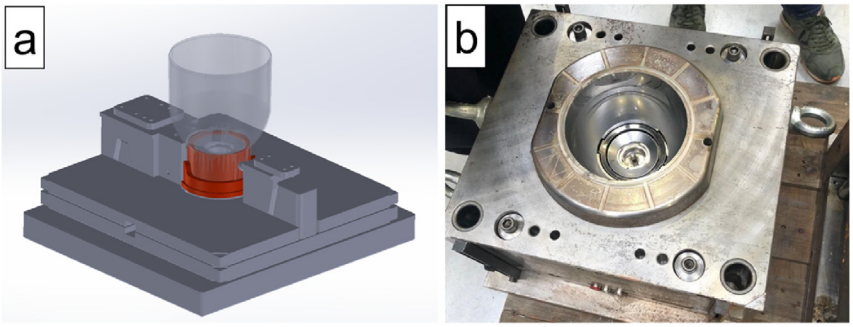

Fig. 3 – (a) 3D model of the insert (in red) in context of some solids of the mould (grey), and a shade representation of the injected part, (b) Detail of the interior of the mould, containing the insert without incorporating conformal cooling channels.

approx.) and thin (10 mm approx.), which complicates the refrigeration in the areas that are the most distant to the mould base. In this context, a hybrid insert [[63]› [54]] is prescribed, having the base to be manufactured via machining operations plus a top-section to be undertaken via L-PBF. The details of this arrangement can be visualised in Fig. 4.

2.2.1. *Design of conformal cooling channels and simulation of the operating conditions*

The base section of the insert includes some machining operations that open standard cooling channels to be utilised with pressurised water. Therefore, new cooling channels in the top section can be connected to those of the base to create a conformal cooling water flow in the top section of the new insert. The geometry of the cooling channels designed is presented in Fig. 5, and it reaches a minimum distance of 3.13 mm to the plastic material to be filled in the mould.

To assess the potential outcomes that could be achieved by the installation of an insert incorporating this CCC design, several simulations (stress, flow and thermal) were undertaken using Moldex3D software (CoreTech System Co., Ltd. (Taiyuan St. Zhubei City, Taiwan)), both with the original insert and to the newly redesigned one. The working conditions for the simulation of the new insert were kept the same as to the ones in the original case; namely: melt temperature of 270 °C, initial mould temperature of 25 °C, cooling medium (water) temperature of 20 °C and 40 °C (at the intake and outtake of the mould). As the first intention with the introduction of the insert was to find a solution to reduce the defect types of breakages during extraction (Type 4), the first simulation maintained the same operating times of the initial case (injection moulding operation to be performed in a total of 105 s, of which 2.8s corresponded to the filling in time, 6s to the packing time, and 75s to cooling time).

The results of the simulation revealed a big potential decrease in temperature of the mould in the areas in contact with the plastic melt, thanks to the most improved cooling behaviour. After 84s of operation, it was reported an important decrease from an initial temperature of approximately 85 °C in the hottest areas to a figure of approximately 40 °C in the same areas in the latter case (see Fig. 6).

2.2.2. *Manufacturing of the insert*

The material removal in the Base section was produced via machining a raw cylindrical inox steel block of material 1.2709 ESU (Uddeholm (Hagfors, Sweden)), capable of working at temperatures from 20 °C to 400 °C. The milling operations were performed in a 3-axis machining centre Deckel Maho DMC 64V linear, (DMG MORI EMEA GmbH (Bielefeld, Germany)). Then, AM L-PBF technology was applied to the top section, using Corrax® AM material (Uddeholm (Hagfors, Sweden)) which has been reported to yield enhanced strength and corrosion resistance on complex hybrid plastic injection moulds [54]. The AM machine utilised was a Selective Laser Melting EOS M290 machine (EOS GmbH (Electro Optical Systems) (Krailling/Munich, Germany)) with a prescribed resolution of 0.03 mm (layer height). According to the material provider specifications, the utilised AM raw material

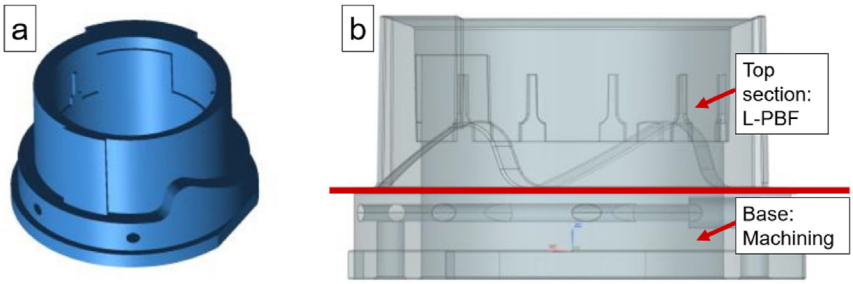

Fig. 4 – Cooling insert geometry and manufacturing process prescription: (a) Isometric view of the design, (b) Differentiation between Top section and Base.

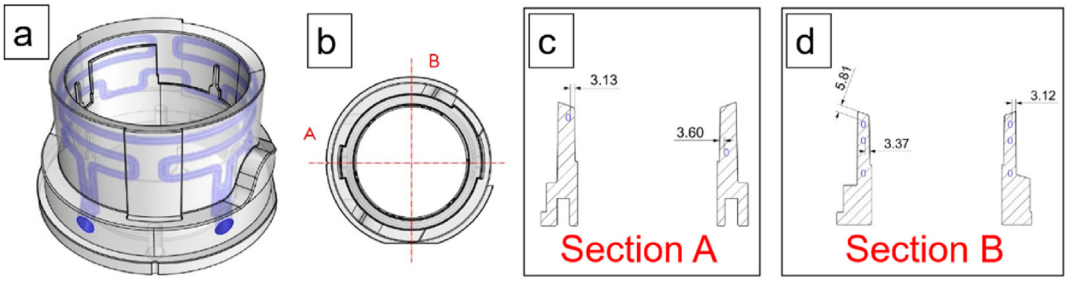

Fig. 5 – (a) Conformal Cooling Channels design, (b) Top view of the insert, (c) Conformal cooling channels distances to the plastic part in section A, (d) Conformal cooling channels distances to the plastic part in section B.

composition contains (wt. %) C (0.03), Si (0.3), Mn (0.3), Cr (12.0), Ni (9.2), Mo (1.4) and Al (1.6).

The utilised machine facilitates an operating construction volume of 250 × 250 × 325 mm^3 and uses as a laser source an Yb fibre laser. The process parameters were set following the material manufacturer indications, i.e.: the laser power was set at 170W, the scanning speed at 1250 mm/s, the scanning strategy was striped with an overlap of 10% from 0.10 mm, and the hatch pattern choice that of a direction of scanning rotated 67° between consecutive layers (default option for DMLS EOS equipment). As the insert had to be completed applying SLM to the previously manufactured base, the natural placement in the construction platform of the machine was placing the base lying flat (in the plane X–Y) and constructing the top section layer-by-layer in the Z-direction (layer height set at 30 μm). The total build time of approximately 70 h for completing the top section of the insert on its raw geometry.

2.2.3. *Post-processing operations*

The insert prepared is to have direct contact with the internal and external surfaces of the injected parts, which will also be visible as the co-polymer raw material utilised is transparent. This implies that before its integration into the mould, the insert requires undergoing several finishing operations. To this respect, the metallic insert geometry after the L-PBF operation presented an excess of material of 1 mm in all the external directions, specially aimed for allowing post-processing operations [64].

The manufactured insert geometry can be easily detached from the construction platform without the need of a cross-cut operation, as the AM process is conducted over the previously machined base (see Fig. 7). At this stage, no defects of cold or incorrect joint between base and top section were reported.

The material excess was removed via postprocessing by finishing milling in the 3-axis machining centre Deckel Maho

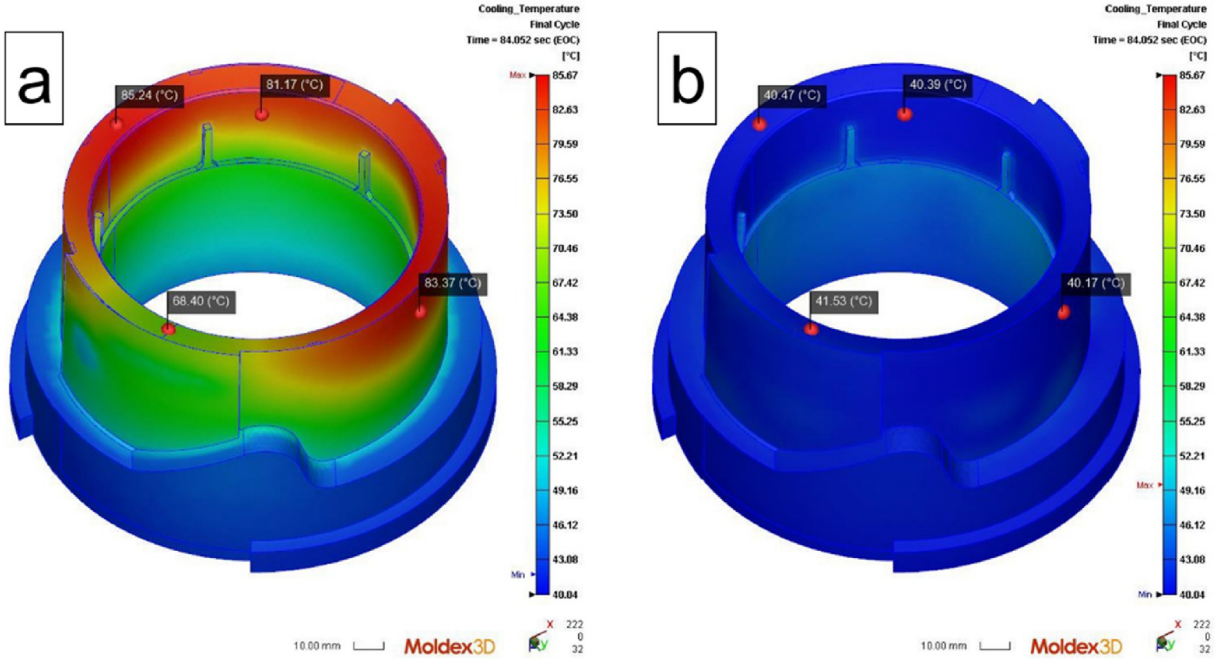

Fig. 6 – (a) Temperature distribution in the contact surface with the plastic melt for the original insert, (b) Temperature distribution in the contact surface with the plastic melt for the final insert design.

DMC 64V linear, (DMG MORI EMEA GmbH (Bielefeld, Germany)) and by electrical discharge machining in an ONA HS400 (ONA Electroerosión S.A. (Durango, Spain)). The as-printed microstructure of the insert is a nickel martensite with about 20% retained austenite. Therefore, the insert was heat-treated with a solution annealing at 850 °C for 30min and then cooled quickly to transform the retained austenite to martensite, and again heat-treated (ageing) for 4 h at 525 °C to achieve a hardness of 50HRC. The cooling was performed leaving the parts in air until they reached the ambient temperature. As anticipated by the material provider, the ageing caused a small and uniform contraction in all the part's directions of 0.07%, which had already been incorporated in the dimensional design of the range of tolerances of the insert. The final geometry is depicted in Fig. 7 (b).

2.3. *Production runs and production data*

To guarantee the meaningfulness of the study, the present analysis includes all production runs undertaken during the period contained between the January 7, 2020 and the July 18, 2022. This period accounted for a total figure of 21 manufacturing orders which were accomplished in 57 different production days. The first 11 manufacturing orders analysed correspond to production before utilising the cooling insert prescribed (total of 31 manufacturing days), whilst the 10 final orders correspond to production after introducing the cooling insert prescribed (total of 26 manufacturing days). The first production date with the new insert was the 6th of July of 2021.

The historical data collected was curated to present the scrap rates generated in the overall and per type of defects analysed in an easy manner and can be retrieved in the Appendix A: **Production data tables** (Tables A1, A2 and A3).

2.4. *Statistical analysis and tests for the goodness of fit*

The statistical analysis undertaken has been performed though the Statistics and Machine Learning Toolbox contained in Matlab 2020b 9.9.0 (The MathWorks, Inc. (Natick, Massachusetts, US)). The data has been treated independently into two subsets that relate to their condition of being obtained before and after the introduction of the insert. For each subset, general statistical parameters have been calculated and compared. The histogram of each subset is assessed against six statistical distributions via three different fit tests to determine whether each candidate distribution could generate the actual data with a very demanding probability of error of maximum 5%. The three fit tests used have been Anderson-Darling, Chi-square, and Kolmogorov-Smirnov, which are useful to assess different characteristics of the data covered. To this regard, Anderson-Darling analyses the differences between the cumulative probability of the data (cumulative number of defects) and that of the proposed distribution (cumulative distribution function). Chi-square calculates a theoretical histogram of the distribution of the actual data, and it compares it with that of the data. Since histograms are a representation of probability density, Chi-square is a test based on the probability of defects. Finally, Kolmogorov-Smirnov is based on the differences between the accumulated probabilities, but unlike Anderson-Darling's, it seeks only the maximum difference, while Anderson-Darling makes a weighted sum of all the differences. Therefore, Anderson-Darling can be more robust than Kolmogorov-Smirnov to outlier (unexpected) data, in which, if there is a single abnormal point, the test is no longer passed.

3. Results and discussion

3.1. *Analysis of the general production scrap rates*

Direct inspection of the time series plot of the Total production Scrap rates over the 57 production days analysed reveals that the introduction of the insert indeed had an impact on the production outcomes (see Fig. 8).

The reduction of the global production scrap rates was an original hypothesis that led to the design and introduction of the cooling insert in the mould. The data reveals a general reduction of rejection rates after the introduction of the insert, as well as a more homogeneous distribution of them. The original hypothesis can therefore be quantified and validated in terms of the variations observed in the Averages and Standard Deviations of the global production scrap rates Before and After the introduction of the insert. Table 1 reflects significant reductions on both parameters (34.3% and 51.9%).

The reduction of the Standard deviation of the global scrap rate is very relevant in the context of the production runs because it narrows the confidence intervals of the required production times, making it possible to schedule tighter production dates. In particular, the planning of the injection moulding production in this industrial case used to incorporate a certain amount of extra time for buffering the defects non-productive time. This means that being capable to prepare more accurate predictions of the real manufacturing times will directly yield higher Overall Equipment Effectiveness (OEE) rates.

With the objective of finding a suitable statistical distribution adjustment, several probability distributions are proposed; namely: Normal, Weibull, Lognormal, Exponential, Pareto Type I, and Beta. As the actual data is processed via histogram, each of these distributions are assessed to analyse each individual goodness of fit (see Fig. 9). Once the statistical distributions are laid, three different fit tests are undertaken to determine whether each candidate distribution could generate the actual data. The plots regarding these statistical distribution function analyses are presented in Figs. 10 and 11, and the outcomes of the statistical distribution normality tests of the global production scrap rates before and after the introduction of the insert for the three calculation methods are presented in Table 2.

3.1.1. *Global scrap ratio before the introduction of the insert*

The level of defects before the introduction of the insert demonstrated a relatively high scrap ratio combined with a high variability. As it can be seen in the data tables in the Appendix and in the figures and tables from previous sections, the maximum scrap rate in the series was a percentage of a 63.38%, whilst the minimum scrap rate was of 4.76%, and the average scrap rate was an 19.05% while its Standard deviation ascended to a 14.16%. These quite large percentages of defects

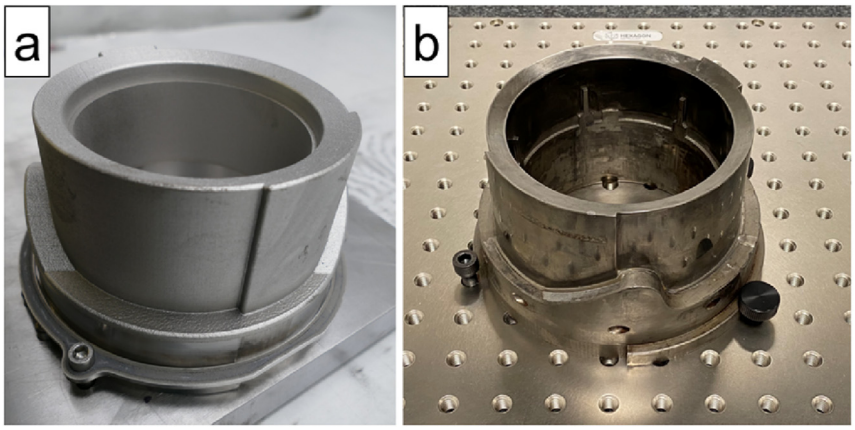

Fig. 7 – Cooling insert object in different stages of its manufacture: (a) Raw geometry obtained by PBF-AM, (b) Insert after undertaking the postprocessing operations (milling and abrasive polishing).

lead to rate the production process as a very inefficient in terms of produced output.

In terms of modelling this behaviour with a statistical distribution, symmetrical arrangements such as the Normal distribution should be avoided due to the nature of the data (negative values of scrap are not expected). From the other 5 distributions evaluated Weibull, Exponential, Pareto, and Beta provide relatively good visual adjustments of both probability, cumulative distribution, as well as in residual results. Concerning the normality tests at 95%, the most well positioned distributions are Exponential and Pareto. As Pareto Type-I can deal well with numerical sets showing large tail areas (probability function decreasing slowly along the occurrence percentage), this distribution is selected for the fit with parameters k = −0.375784 [−0.645299, −0.106269] and σ = 0.278744 [0.182572, 0.425577], corresponding to the parameters of scale and shape of such statistical distribution.

3.1.2. *Global scrap ratio after the introduction of the insert*

The level of defects after the introduction of the insert demonstrates a relatively lower scrap ratio than in the previous case, combined with a lower variability. As it can be seen from the data, the maximum scrap rate in the series was a percentage of a 28.80%, whilst the minimum scrap rate was of 3.70%, and the average scrap rate was an 14.21% while its Standard deviation was kept to a 6.81%. In this case, these percentages lead to rate the production process as more efficient in terms of output.

In terms of modelling this behaviour with a statistical distribution, symmetrical arrangements such as the Normal distribution should also be avoided due to the nature of the data (negative values of scrap are still not expected). From the other 5 distributions evaluated, only Weibull, Lognormal, and Beta provide relatively good visual adjustments for probability and cumulative distribution. Concerning the normality tests at 95%, the 3 distributions Weibull, Lognormal, and Beta are properly positioned to provide suitable models. Considering the adjustment of residual results, a Weibull distribution fit with parameters A = 0.152798 [0.126595, 0.184426] and B = 2.15907 [1.60207, 2.90972] is selected as the best proxy for the process after the introduction of the insert, being A the scale and B the shape parameters of such distribution.

3.2. *Analysis of scrap rates per type of defect*

The statistical analysis of the variation of scrap rates per type of defect before and after the introduction of the insert has again been conducted via the main statistical indicators

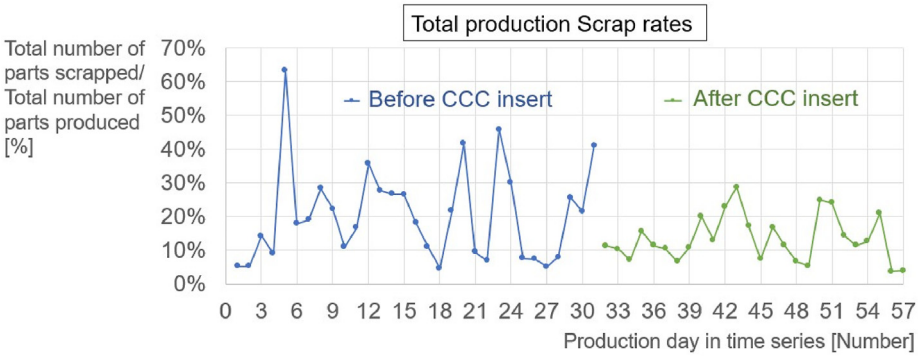

Fig. 8 – Time series plot of the Total production Scrap rates over the 57 production runs analysed.

Table 1 – Averages and Standard deviations of the global production scrap rates Before and After the introduction of the insert and their associated variation rates.

Global Production Scrap rates	Average	Standard deviation
Before insert	20.53%	14.16%
After insert	13.48%	6.81%
Variation rates	−34.3%	−51.9%

(Averages and Standard deviations, see Table 3) and as the best fit to a statistical distribution (See Fig. 12). The main findings are described in the following sections.

3.2.1. *Surface defects scrap rates analysis (defect type 1)*
In terms of relative occurrence, the superficial defects were the most common type of defect in the initial production settings, accounting for a total average of an 8.95% of defects reported in the period. Before the introduction of the insert, the Standard deviation of the occurrence of this type of defect was also relatively high, accounting for a figure of a 7.35%. However, once the insert was installed, both Average and Standard deviation figures for the scrap rates reduced dramatically to levels approximately half of the initial ones (see Table 3). Concerning the statistical adjustment, comparing the histograms for the cases before and after the introduction of the insert, it can be inferred that the same distribution adjustment that in the global case can be made for this type of defect (i.e.: Pareto Type-I for the former, and Weibull for the latter). This information is presented graphically in Fig. 12.

3.2.2. *Integrity scrap rates analysis (defect type 2)*
Regarding integrity (Type 2 defects), this was a sort of deficiency that bore the least percentage of occurrence (average of 2.92%), and it is the only one that has experienced and increase on the percentage of occurrence after the introduction of the L-PBF conformal cooling insert (up to a 5.39%), taking the lead in the type of defects encountered. Contrarily, the variability of such defect rates decreased with the incorporation of the insert in the mould, departing from a rate of 5.58% down to a rate of 3.55% (See Table 3). Regarding the statistical adjustment, comparing the histograms for the cases before and after the introduction of the insert, Pareto Type-I and Weibull keep generating a good level of visual fit. This information can be retrieved graphically in Fig. 12.

3.2.3. *Incomplete fill-in scrap rates analysis (defect type 3)*
Concerning Incomplete fill-in, this type of defect (Type 3) was the second least in terms of occurrence, prior to the incorporation of the insert in the mould (accounting for a 3.33% of the produced parts). Besides, the Standard Deviation, with a value of 4.43% was the smallest contemplated in the 4 types of defects. To this respect, once the insert was incorporated to the mould, the variation of both figures was almost unperceivable, with variation rates of 0.86% and 0.02% respectively (See Table 3). Then, with regards to the statistical adjustment, comparing the histograms for the cases before and after the introduction of the insert, there is no impediment to select the same Pareto Type-I and Weibull distributions with a good level of visual fit (See Fig. 12).

3.2.4. *Breakages during extraction scrap rates analysis (defect type 4)*
The final type of defects analysed is the one that originated the case study, namely breakages of parts during mould extraction. Concerning this (Type 4), the average level of occurrence before and after revealed a decrease of two thirds of the initial scrap rates for the produced parts (from 3.85% to 1.79%), validating in this way the original hypothesis that PBF AM produced parts can help in controlling and fixing the temperature levels in different sections of the moulds. Also, the Standard deviation of the latter scrap rates revealed to be significantly smaller than the formerly observed percentages (from 12.52% to 2.92%). This information is presented in Table 3. Concerning to the statistical adjustment, again, comparing the histograms for the cases before and after the introduction of the insert, same Pareto Type-I and Weibull distributions can be selected from the visual fit (See Fig. 12).

3.3. *Confidence interval for the global scrap rate*

On the one hand, the confidence interval for the global scrap rate for the situation before the introduction of the insert can be calculated in terms of the Pareto-Type I adjusted

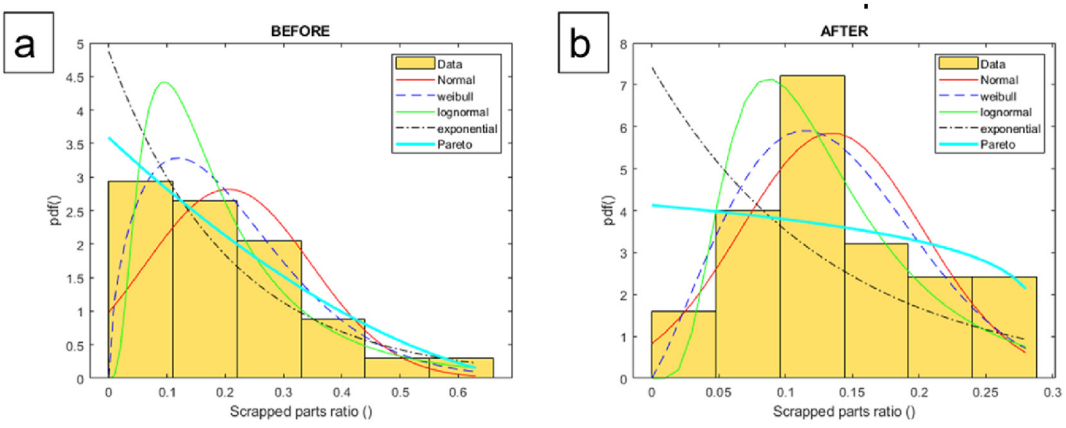

Fig. 9 – Global scrap rates histogram fit for the 6 distributions assessed: (a) before the introduction of the insert, and (b) after the introduction of the insert.

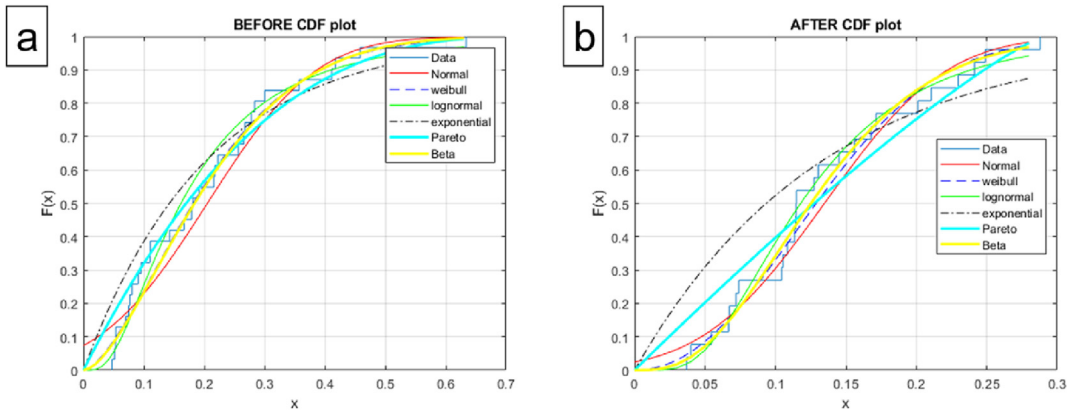

Fig. 10 – Cumulative Distribution Function plots: (a) before the introduction of the insert, and (b) after the introduction of the insert.

distribution, which for a production run of 100 parts leads to an estimated number of defects between 10% and 28%, being the most probable situation a yield of 17% of scrap (see Fig. 13 (a)). This means that in the former case, the production planning, if conservative, should had been undertaken foreseeing the time expected for manufacturing 128 parts. On the other hand, the confidence interval for the global scrap rate for the situation after the introduction of the insert can be calculated in terms of the Weibull adjusted distribution, which for a production run of 100 parts leads to a quantity of defects between 10% and 16%, being the most likely outcome to produce a 13% of scrap parts (see Fig. 13 (b)). This means that in the latter case, the production planning, if conservative, should had been undertaken foreseeing the time expected for manufacturing 116 parts. These results yield that the introduction of the L-PBF CCC insert has been able to decrease the estimated production time by a percentage of 12% in the most favourable estimate, and by a percentage of a 4% in the most probable case during the studied periods.

3.4. *L-PBF as an enhancer of the reduction of scrap rates*

Once the statistical analysis of the results over a time series of real manufacturing data has been completed, and the comparison framework has been established, it is also noteworthy to assess how the L-PBF process has acted as an enhancer of the reduction of scrap rates and to draft how have its technical properties helped towards this direction.

3.4.1. *Comparison between cooling enhancement rates (before and after)*

The freedom of design of the channels, which allows a fine adjustment of the temperature distribution in critical places of the mould operation, had demonstrated in the past potential to reduce cycle times and to increase production volumes. In the present case, the simulations undertaken using Moldex3D software (CoreTech System Co., Ltd. (Taiyuan St. Zhubei City, Taiwan)), comparing the original insert with the newly redesigned one

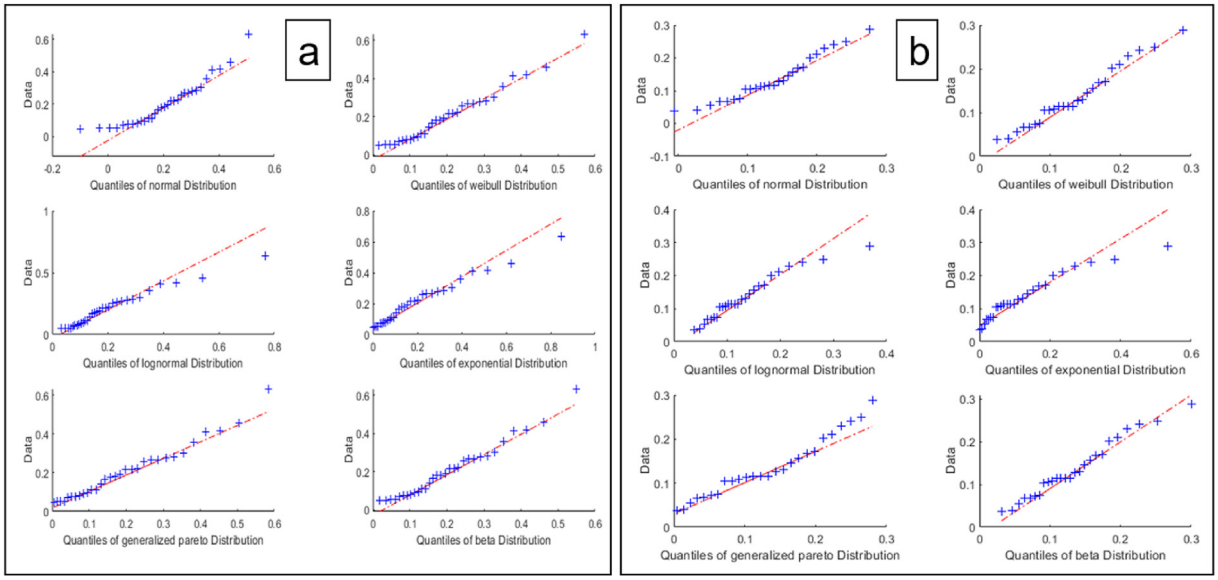

Fig. 11 – Residual plots for each of the statistical distributions (Normal, Weibull, Lognormal, Exponential, Pareto, and Beta) evaluated in the cases (a) before and (b) after the introduction of the insert.

Table 2 – Outcomes of the statistical distribution normality tests at a probability of 95% of the global production scrap rates Before and After the introduction of the insert for the three calculation methods.

	Before the introduction of the insert			After the introduction of the insert		
Statistical Distribution	Anderson-Darling	Chi-Square	Kolmogorov-Smirnov	Anderson-Darling	Chi-Square	Kolmogorov-Smirnov
Normal	Fail	Fail	Fail	Fail	Fail	Fail
Weibull	Fail	Fail	Fail	Fail	Fail	Pass
Lognormal	Fail	Fail	Fail	Pass	Fail	Pass
Exponential	Pass	Fail	Pass	Pass	Fail	Pass
Pareto	Fail	Fail	Pass	Pass	Fail	Pass
Beta	Fail	Fail	Fail	Fail	Fail	Pass

Table 3 – Averages and Standard deviations of the production scrap rates caused by the 4 types of defects analysed Before and After the introduction of the insert and their associated variation rates.

	Defect type 1 (Surface)		Defect type 2 (Integrity)		Defect type 3 (Incomplete fill-in)		Defect type 4 (Breakages)	
Production Scrap rates	Average	Standard deviation	Average	Standard deviation	Average	Standard deviation	Average	Standard deviation
Before insert	8.95%	7.35%	2.92%	5.58%	3.33%	4.43%	3.85%	12.52%
After insert	4.19%	4.03%	5.39%	3.55%	4.19%	4.44%	1.79%	2.92%
Variation rates	−4.76%	−3.32%	2.47%	−2.03%	0.86%	0.02%	−2.06%	−9.61%

depict an average Temperature reduction of a 37.2% in the interior and a 46.8% on the surface. This functioning mode leads to a 34.9% of average temperature reduction on the interior of the injected part, and up to a 39.3% on its surface. The detail of this data can be retrieved in Table A4 of Appendix A.

3.4.2. *Cost assessment of the introduction of AM CCCs*

The Initial investment including the simulation, manufacturing, postprocessing and installation of the new insert in the mould accounted for a total of 4643.89€. Considering that the costs induced by a scrapped part are of 5.52€, the investment break-even is achieved when 842 parts are saved from scrapping. The total number of parts produced in the 26 days with production after introducing the new insert accounted for 12,529. As the absolute reduction of the total scrap rate was of 7.05%, it can be considered that a total of 883 parts were saved from being scrapped comparing to the former situation, which means that the break-even was achieved during the period.

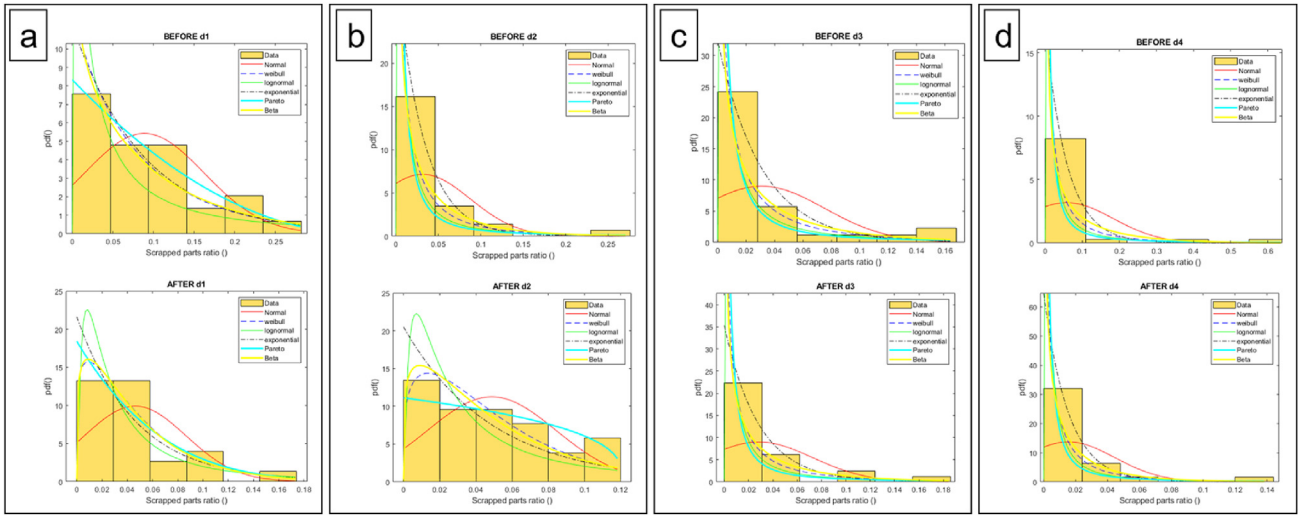

Fig. 12 – Scrap rates histogram fit for the 6 distributions assessed before the introduction of the insert for the 4 defect types analysed: (a) Surface, (b) Integrity, (c) Incomplete fill-in, and (d) Breakages.

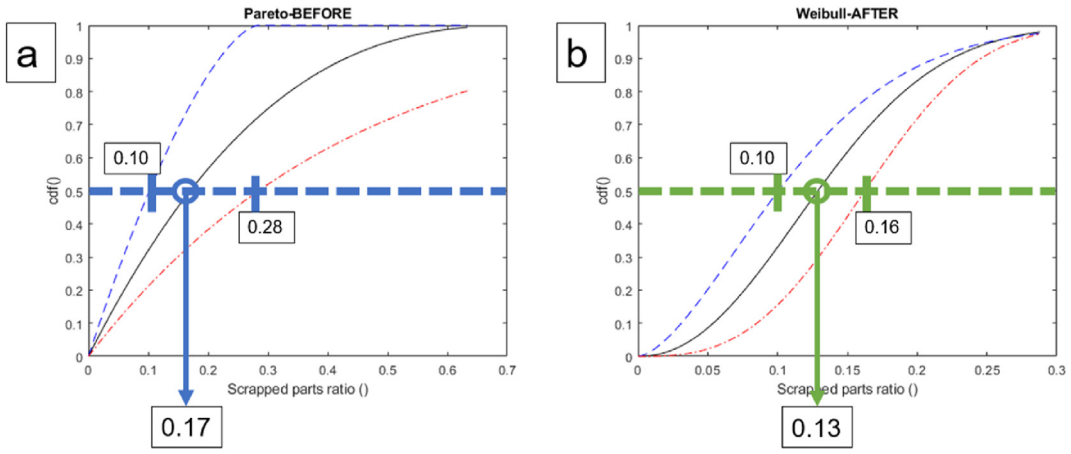

Fig. 13 – Cumulative distribution of defects for the two statistical distributions fit: (a) Pareto I-Before, and (b) Weibull-After.

Additionally, the total number of parts accepted from the January 7, 2020 until the July 18, 2022 (total of 2.53 calendar years) was of 22,872, which corresponds to an equivalent of 9040 parts per calendar year. With this average, and taking into account the most probable reduction of parts needed to be produced of a 4%, the expected savings would be of 1996.10€ per calendar year, whilst if taking the most favourable estimation of the reduction of parts needed to be produced (12%), the expected savings could be of 5988.31€ in a calendar year (an amount corresponding to 0.78 times the initial investment; meaning it could pay back in only 9.3 months).

3.4.3. *Design considerations of the AM CCCs introduced*

Concerning the design of the AM CCC introduced, several considerations have had to be respected during its development. Firstly, all channels are compliant with a safety distance between them and any outer skin surface of 3 mm. This is of interest for the integrity of the insert and to ensure that the channels will not collapse when the mould is in operation. Also, there cannot be internal sharp edges in the channels to avoid the cavitation phenomena, and the flow velocity must ensure a sufficiently high Reynolds coefficient to maintain a turbulent regime. This set of prescriptions compromise what features are feasible from the design point of view and impose restrictions on the performance that can be obtained and about how can a certain temperature distribution and extreme values be achieved.

4. Conclusions

The initial hypothesis of the redesign is confirmed (global scrap rates are reduced with the introduction of the L-PBF AM conformal cooling insert, from 20.53% to 13.48%; reduction of 7.05%). Additionally, Standard deviation of the global scrap rate is also found to be reduced (from 14.16% to 6.81%; reduction of a 7.35%), which is very remarkable for the production runs as possibilities to narrow the confidence intervals of the manufacturing runs and thus making possible to schedule tighter production dates.

Concerning the global scrap rates before the introduction of the insert, the best statistical fit is found utilising a statistical distribution Pareto Type-I. Once the insert is introduced in the mould, the best statistical fit found is with a Weibull distribution, which has a much narrower dispersion of the results.

Regarding the analysis for each of the four different product defect types, the results reveal a specific decrease on the average occurrence of two of them, namely: superficial (−4.76%), and breakages during extraction (−2.06%)), as well as a specific decrease in the variability of their occurrence rates in three of them (optical (−3.32%), part integrity (−2.03%), and breakages during extraction (−9.61%)). This means that, apart from reducing the scrap rates generated by breakages during extractions, the introduction of L-PBF AM conformal cooling insert can also yield benefits in terms of optical defects and integrity, without compromising the defect rates generated by incomplete filling-in.

Finally, because of the characterisation of the new process adjusting a Weibull distribution function, the confidence intervals for the global scrap rates in future production runs makes it possible reduce the estimated production time by a percentage of a 12% in the most favourable estimate, and by a percentage of a 4% in the most probable case during the studied periods.

Author contributions

Conceptualization, J.M.-C. and S.M.P.; methodology, J.M.-C. and S.M.P.; software, J.M.-C., S.M.P. and V.CdM.I.; validation, J.M.-C. and MA.dlS.-L.; formal analysis, J.M.-C., V.CdM.I. and M.A.dlS.-L.; investigation, J.M.-C., V.CdM.I. and S.M.P.; resources, S.M.P.; data curation, J.M.-C. and V.CdM.I.; writing-original draft preparation, J.M.-C.; writing-review and editing, J.M.-C. and S.M.P.; visualization, J.M.-C. and V.CdM.I.; supervision, MA.dlS.-L.; project administration, S.M.P.; funding acquisition, S.M.P. and MA.dlS.-L.. All authors have read and agreed to the published version of the manuscript.

Funding

This research was partially funded by ACCIÓ (Agència de la Competitivitat Empresarial de la Generalitat de Catalunya) under project PRO2: "Ecosistemes d'R + D + I per la implementació i adopció de la Fabricació Additiva/impressió 3D a la fabricació de productes industrials i als processos industrials de producció", grant number COMRDI16-1-0009 (Projecte R + D Comunitats RIS3CAT). This project is co-financed by the European Regional Development Fund of the European Union within the framework of the Programa Operatiu FEDER de Catalunya 2014–2020. The authors Joaquim Minguella-Canela and Vicente César de Medina Iglesias are Serra Húnter Fellows. The APC were covered with own funds.

Declaration of competing interest

The authors declare that they have no known competing financial interests or personal relationships that could have appeared to influence the work reported in this paper.

Acknowledgements

The authors would like to acknowledge the valuable simulations and technical information provided by Alberto Santana from voestalpine High Performance Metals Iberia S.A.U., Chen (Gary) Kuan Ying from voestalpine Technology Institute (Asia) Co. Ltd. And Jens Christoffel from voestalpine Additive Manufacturing Centre GmbH. (Dusseldorf).

Appendix A: Production and simulation data tables

Table A1 – Production runs, dates and total scrap generated before and after the introduction of the Conformal Cooling AM insert.

	Production run	Production Date	Num. Total Parts Produced	Num. Total Parts Scrapped	% Total Parts Scrapped
Production runs before Conformal Cooling AM insert introduction	1	07/01/2020	337	18	5,34%
	2	08/01/2020	771	41	5,32%
	3	09/01/2020	728	104	14,29%
	4	10/01/2020	484	44	9,09%
	5	27/02/2020	142	90	63,38%
	6	28/02/2020	764	137	17,93%
	7	18/03/2020	261	50	19,16%
	8	19/03/2020	733	208	28,38%
	9	20/03/2020	736	164	22,28%
	10	23/03/2020	245	27	11,02%
	11	24/03/2020	738	123	16,67%
	12	25/03/2020	344	123	35,76%
	13	15/10/2020	72	20	27,78%
	14	16/10/2020	811	217	26,76%
	15	19/10/2020	614	163	26,55%
	16	09/11/2020	127	23	18,11%
	17	10/11/2020	631	70	11,09%
	18	11/01/2021	273	13	4,76%
	19	12/01/2021	731	159	21,75%
	20	13/01/2021	357	149	41,74%
	21	03/03/2021	345	33	9,57%
	22	04/03/2021	615	43	6,99%
	23	21/04/2021	192	88	45,83%
	24	22/04/2021	669	201	30,04%
	25	23/04/2021	535	41	7,66%
	26	10/05/2021	280	21	7,50%
	27	11/05/2021	659	34	5,16%
	28	12/05/2021	298	24	8,05%
	29	08/06/2021	273	70	25,64%
	30	09/06/2021	736	159	21,60%
	31	10/06/2021	474	195	41,14%
Production runs after Conformal Cooling AM insert introduction	32	06/07/2021	352	40	11,36%
	33	07/07/2021	824	86	10,44%
	34	08/07/2021	403	29	7,20%
	35	24/08/2021	679	106	15,61%
	36	25/08/2021	236	27	11,44%
	37	19/10/2021	57	6	10,53%

(continued on next page)

Table A1 – (*continued*)

	Production run	Production Date	Num. Total Parts Produced	Num. Total Parts Scrapped	% Total Parts Scrapped
	38	20/10/2021	**669**	45	6,73%
	39	21/10/2021	**701**	76	10,84%
	40	22/10/2021	**358**	72	20,11%
	41	11/11/2021	**299**	39	13,04%
	42	12/11/2021	**683**	157	22,99%
	43	19/01/2022	**382**	110	28,80%
	44	20/01/2022	**700**	120	17,14%
	45	21/01/2022	**635**	47	7,40%
	46	14/03/2022	**375**	63	16,80%
	47	15/03/2022	**828**	95	11,47%
	48	16/03/2022	**583**	39	6,69%
	49	23/05/2022	**275**	15	5,45%
	50	24/05/2022	**494**	123	24,90%
	51	25/05/2022	**808**	195	24,13%
	52	26/05/2022	**365**	53	14,52%
	53	04/07/2022	**235**	27	11,49%
	54	05/07/2022	**715**	91	12,73%
	55	06/07/2022	**494**	104	21,05%
	56	15/07/2022	**54**	2	3,70%
	57	18/07/2022	**325**	13	4,00%
		Total	**27504**	**4632**	**16,84%**

Table A2 – Production runs, and scrap generated per type of defect before the introduction of the Conformal Cooling AM insert.

	Production run	Num. Optical defects (Type 1)	% Optical defects (Type 1)	Num. Integri-ty defects (Type 2)	% Intergi-ty defects (Type 2)	Num. Incom-plete fill-in defects (Type 3)	% Incom-plete fill-in defects (Type 3)	Num. Broken when extracting defects (Type 4)	% Broken when extracting defects (Type 4)
Production runs before Conformal Cooling AM insert introduction	1	2	0,6%	8	2,4%	8	2,4%	0	0,0%
	2	22	2,9%	12	1,6%	4	0,5%	3	0,4%
	3	51	7,0%	9	1,2%	23	3,2%	21	2,9%
	4	20	4,1%	2	0,4%	0	0,0%	22	4,5%
	5	0	0,0%	0	0,0%	0	0,0%	90	63,4%
	6	0	0,0%	40	5,2%	41	5,4%	56	7,3%
	7	0	0,0%	35	13,4%	0	0,0%	15	5,7%
	8	162	22,1%	6	0,8%	13	1,8%	27	3,7%
	9	146	19,8%	3	0,4%	15	2,0%	0	0,0%
	10	12	4,9%	0	0,0%	0	0,0%	15	6,1%
	11	85	11,5%	2	0,3%	29	3,9%	7	0,9%
	12	74	21,5%	0	0,0%	49	14,2%	0	0,0%
	13	11	15,3%	4	5,6%	5	6,9%	0	0,0%
	14	58	7,2%	25	3,1%	132	16,3%	2	0,2%
	15	66	10,7%	52	8,5%	11	1,8%	34	5,5%
	16	20	15,7%	0	0,0%	3	2,4%	0	0,0%
	17	66	10,5%	0	0,0%	0	0,0%	4	0,6%
	18	11	4,0%	0	0,0%	0	0,0%	2	0,7%
	19	102	14,0%	0	0,0%	36	4,9%	21	2,9%
	20	100	28,0%	21	5,9%	10	2,8%	18	5,0%
	21	29	8,4%	4	1,2%	0	0,0%	0	0,0%
	22	40	6,5%	3	0,5%	0	0,0%	0	0,0%
	23	24	12,5%	0	0,0%	0	0,0%	64	33,3%
	24	78	11,7%	11	1,6%	6	0,9%	106	15,8%
	25	41	7,7%	0	0,0%	0	0,0%	0	0,0%
	26	6	2,1%	0	0,0%	0	0,0%	15	5,4%
	27	1	0,2%	1	0,2%	2	0,3%	30	4,6%
	28	2	0,7%	1	0,3%	0	0,0%	21	7,0%
	29	12	4,4%	26	9,5%	32	11,7%	0	0,0%
	30	39	5,3%	44	6,0%	74	10,1%	2	0,3%
	31	60	12,7%	128	27,0%	6	1,3%	1	0,2%

Table A3 – Production runs, and scrap generated per type of defect after the introduction of the Conformal Cooling AM insert.

	Production run	Num. Optical defects (Type 1)	% Optical defects (Type 1)	Num. Integri-ty defects (Type 2)	% Intergi-ty defects (Type 2)	Num. Incom-plete fill-in defects (Type 3)	% Incom-plete fill-in defects (Type 3)	Num. Broken when extracting defects (Type 4)	% Broken when extracting defects (Type 4)
Production runs atfer Conformal Cooling AM insert introduction	32	14	4,0%	8	2,3%	9	2,6%	9	2,6%
	33	27	3,3%	36	4,4%	2	0,2%	21	2,5%
	34	29	7,2%	0	0,0%	0	0,0%	0	0,0%
	35	27	4,0%	13	1,9%	66	9,7%	0	0,0%
	36	19	8,1%	8	3,4%	0	0,0%	0	0,0%
	37	5	8,8%	1	1,8%	0	0,0%	0	0,0%
	38	17	2,5%	1	0,1%	26	3,9%	1	0,1%
	39	30	4,3%	4	0,6%	5	0,7%	37	5,3%
	40	14	3,9%	9	2,5%	38	10,6%	11	3,1%
	41	15	5,0%	24	8,0%	0	0,0%	0	0,0%
	42	35	5,1%	80	11,7%	41	6,0%	1	0,1%
	43	11	2,9%	29	7,6%	70	18,3%	0	0,0%
	44	8	1,1%	69	9,9%	42	6,0%	1	0,1%
	45	3	0,5%	40	6,3%	1	0,2%	3	0,5%
	46	42	11,2%	20	5,3%	1	0,3%	0	0,0%
	47	3	0,4%	92	11,1%	0	0,0%	0	0,0%
	48	7	1,2%	31	5,3%	0	0,0%	1	0,2%
	49	2	0,7%	10	3,6%	3	1,1%	0	0,0%
	50	85	17,2%	2	0,4%	29	5,9%	7	1,4%
	51	21	2,6%	62	7,7%	1	0,1%	111	13,7%
	52	7	1,9%	17	4,7%	13	3,6%	16	4,4%
	53	10	4,3%	13	5,5%	0	0,0%	4	1,7%
	54	33	4,6%	53	7,4%	5	0,7%	0	0,0%
	55	55	11,1%	49	9,9%	0	0,0%	0	0,0%
	56	0	0,0%	1	1,9%	0	0,0%	1	1,9%
	57	6	1,8%	3	0,9%	4	1,2%	0	0,0%

Table A4 – Simulated results for the evolution of the Temperature distributions (internal and superficial) of the insert and of the part, before and after the incorporation of Conformal Cooling Channels.

	Before incorporating CCC		After incorporating CCC		Average Temp. Reduction	
	T Max. [ºC]	T Min. [ºC]	T Max. [ºC]	T Min. [ºC]	Average [ºC]	Ratio [%]
Insert internal temperature distribution	83,36	49,08	43,03	40,19	24,61	37,2%
Insert surface temperature distribution	85,24	68,40	41,53	40,17	35,97	46,8%
Part interior temperature distribution	83,26	60,54	52,31	41,31	25,09	34,9%
Part surface temperature distribution	85,24	67,17	52,02	40,45	29,97	39,3%

REFERENCES

[1] Phull GP, Kumar S, Walia RS. Conformal cooling for molds produced by additive manufacturing: a review. Int J Mech Eng Technol 2018;9(1):1162–72.

[2] Moshiri M, Tosello G, Mohanty S. Defects investigation in additively manufactured steel products for injection moulding. Euro PM2018 Congress Proceedings. 2018. p. 6. ISBN (Electronic) 978-1-899072-50-7.

[3] Meckley J, Edwards R. A study on the design and effectiveness of conformal cooling channels in rapid tooling inserts. Technol. Interface Journal/Fall. 2009;10(1):1–28.

[4] Shayfull Z, Sharif S, Zain AM, Ghazali MF, Saad RM. Potential of conformal cooling channels in rapid heat cycle molding: a review. Adv Polym Technol 2014;33(1). https://doi.org/10.1002/adv.21381.

[5] Shine MS, Ashtankar KM, Kuthe AM, Dahake SW, Mawale MB. Direct rapid manufacturing of molds with conformal cooling channels. Rapid Prototyp J 2018;24(8):1347–64. https://doi.org/10.1108/RPJ-12-2016-0199.

[6] Kanbur BB, Shen S, Duan F. Design and optimization of conformal cooling channels for injection molding: a review. Int J Adv Manuf Technol 2020;106:3253–71. https://doi.org/10.1007/s00170-019-04697-9.

[7] Brøtan V, Åsebø Berg O, Sørby K. Additive manufacturing for enhanced performance of molds. Procedia CIRP 2016;54:186–90. https://doi.org/10.1016/j.procir.2016.05.074.

[8] Ferro P, Meneghello R, Savio G, Berto F. A modified volumetric energy density–based approach for porosity assessment in additive manufacturing process design. Int J

Adv Manuf Technol 2020;1107(110):1911–21. https://doi.org/10.1007/S00170-020-05949-9.
[9] Shinde MS, Ashtankar KM. Additive manufacturing–assisted conformal cooling channels in mold manufacturing processes. Adv Mech Eng 2017;9(5):1–14. https://doi.org/10.1177/1687814017699764.
[10] Kampker A, Triebs J, Kawollek S, Ayvaz P, Beyer T. Direct polymer additive tooling – effect of additive manufactured polymer tools on part material properties for injection moulding. Rapid Prototyp J 2019;25(10):1575–84. https://doi.org/10.1108/RPJ-07-2018-0161.
[11] Hofstätter T, Bey N, Mischkot M, Lunzer A, Pedersen DB, Norgaard Hansen H. Comparison of conventional injection mould inserts to additively manufactured inserts using life cycle assessment. Nottingham, UK: euspen's 16th International Conference & Exhibition; May 2016.
[12] Gohn AM, Brown D, Mendis G, Forster S, Rudd N, Giles M. Mold inserts for injection molding prototype applications fabricated via material extrusion additive manufacturing. Addit Manuf 2022;51:102595. https://doi.org/10.1016/j.addma.2022.102595.
[13] Frazier WE. Metal additive manufacturing: a review. J Mater Eng Perform 2014;23(6):1917–28. https://doi.org/10.1007/s11665-014-0958-z.
[14] Gao W, Zhang Y, Ramanujan D, Ramani K, Chen Y, Williams CB, et al. The status, challenges, and future of additive manufacturing in engineering. Comput Aided Des 2015;69:65–89. https://doi.org/10.1016/j.cad.2015.04.001.
[15] Wang D, Song C, Yang Y, Liu R, Ye Z, Xiao D, Liu Y. Research on the redesign of precision tools and their manufacturing process based on selective laser melting (SLM). Rapid Prototyp J 2016;22(1):104–14. https://doi.org/10.1108/RPJ-02-2014-0021.
[16] Depboylu FN, Yasa E, Poyraz Ö, Minguella-Canela J, Korkusuz F, De los Santos López MA. Titanium based bone implants production using laser powder bed fusion technology. J Mater Res Technol 2022;17:1408–26. https://doi.org/10.1016/j.jmrt.2022.01.087.
[17] Asgari H, Mohammadi M. Microstructure and mechanical properties of stainless steel CX manufactured by Direct Metal Laser Sintering. Mater Sci Eng 2018;709:82–9. https://doi.org/10.1016/j.msea.2017.10.045.
[18] Feng S, Kamat AM, Pei Y. Design and fabrication of conformal cooling channels in molds: review and progress updates. Int J Heat Mass Tran 2021;171:121082. https://doi.org/10.1016/j.ijheatmasstransfer.2021.121082.
[19] Vasco J, Barreiros FM, Nabais A, Reis N. Additive manufacturing applied to injection moulding: technical and economic impact. Rapid Prototyp J 2019;25(7):1241–9. https://doi.org/10.1108/RPJ-07-2018-0179.
[20] Mazur M, Brincat P, Leary M, Brandt M. Numerical and experimental evaluation of conformally cooled H13 steel injection mould manufactured with selective laser melting. Int J Adv Manuf Technol 2017;93:881–900. https://doi.org/10.1007/s00170-017-0426-7.
[21] Ganesh DG, Sarang SC, Sai MJ. Design, optimization and validation of conformal cooling technique for additively manufactured mold insert. J Phys: Conf. Ser. 2021;2070:012225. https://doi.org/10.1088/1742-6596/2070/1/012225.
[22] Kirchheim A, Katrodiya Y, Zumofen L, Ehrig F, Wick C. Dynamic conformal cooling improves injection molding. Hybrid molds manufactured by laser powder bed fusion. Int J Adv Manuf Technol 2021;114:107–16. https://doi.org/10.1007/s00170-021-06794-0.
[23] Kanbur BB, Zhou Y, Shen S, Wong KH, Chen C, Shocket A, et al. Metal additive manufacturing of plastic injection molds with conformal cooling channels. Polymers 2022;14:424. https://doi.org/10.3390/polym14030424.
[24] Klahn C, Leutenecker B, Meboldt M. Design for additive manufacturing – supporting the substitution of components in series products. Procedia CIRP 2014;21:138–43. https://doi.org/10.1016/j.procir.2014.03.145.
[25] Minguella-Canela J, Morales Planas S, De los Santos-López MA. SLM manufacturing redesign of cooling inserts for high production steel moulds and benchmarking with other industrial additive manufacturing strategies. Materials 2020;13:4843. https://doi.org/10.3390/ma13214843.
[26] Asnafi N, Rajalampi J, Aspenberg D, Alveflo A. Production tools made by additive manufacturing through laser-based powder bead fusion. Berg Huettenmaenn Mon 2020;165(3):125–36. https://doi.org/10.1007/s00501-020-00961-8.
[27] Kruth JP, Froyen L, Van Vaerenbergh J, Mercelis P, Rombouts M, Lauwers B. Selective laser melting of iron-based powder. J Mater Process Technol 2004;149:616–22. https://doi.org/10.1016/J.JMATPROTEC.2003.11.051.
[28] Osakada K, Shiomi M. Flexible manufacturing of metallic products by selective laser melting of powder. Int J Mach Tool Manufact 2006;46:1188–93. https://doi.org/10.1016/J.IJMACHTOOLS.2006.01.024.
[29] Yadroitsev I, Thivillon L, Bertrand P, Smurov I. Strategy of manufacturing components with designed internal structure by selective laser melting of metallic powder. Appl Surf Sci 2007;254(4):980–3. https://doi.org/10.1016/j.apsusc.2007.08.046.
[30] Razavi S, Bordonaro G, Ferro P, Torgersen J, Berto F. Fatigue behavior of porous Ti-6Al-4V made by laser-engineered net shaping. Materials 2018;11:284. https://doi.org/10.3390/ma11020284.
[31] 3DSystems, Machine DMP Flex 350, https://es.3dsystems.com/3d-printers/dmp-flex-350.
[32] Dalgarno KW, Stewart TD. Manufacture of production injection mould tooling incorporating conformal cooling channels via indirect selective laser sintering. Proc Inst Mech Eng Part B J Eng Manuf 2001;215:1323–32. https://doi.org/10.1243/0954405011519042.
[33] Klingaa CG, Bjerre MK, Baier S, De Chiffre L, Mohanty S, Hattel JH. Roughness investigation of SLM manufactured conformal cooling channels using X-ray computed tomography. In: Proc. 9th conf. Ind. Comput. Tomogr.; 2019. p. 1–10. Padova, Italy.
[34] Liu C, Cai Z, Dai Y, Huang N, Xu F, Lao C. Experimental comparison of the flow rate and cooling performance of internal cooling channels fabricated via selective laser melting and conventional drilling process. Int J Adv Manuf Technol 2018;96:2757–67. https://doi.org/10.1007/s00170-018-1799-y.
[35] Hsue AWJ, Pan YD, Lu LW. A novel string-bead EDM mechanism for dressing of the conformal cooling channel fabricated by the SLM-additive manufacture. J Phys Conf 2021;2020:012035. https://doi.org/10.1088/1742-6596/2020/1/012035. IOP Publishing.
[36] Lee J-Y, Nagalingam AP, Yeo SH. A review on the state-of-the-art of surface finishing processes and related ISO/ASTM standards for metal additive manufactured components. Virtual Phys Prototyp 2021;16:68–96. https://doi.org/10.1080/17452759.2020.1830346.
[37] Wüst P, Edelmann A, Hellmann R. Areal surface roughness optimization of maraging steel parts produced by hybrid additive manufacturing. Materials 2020;13:418. https://doi.org/10.3390/ma13020418.
[38] Solakoğlu EU, Gürgen S, Kuşhan MC. Surface topography of nickel-based superalloy manufactured with direct metal

laser sintering (DMLS) method. Surf Topogr Metrol Prop 2019;7:015012. https://doi.org/10.1088/2051-672X/aafe33.
[39] Jamshidinia M, Kovacevic R. The influence of heat accumulation on the surface roughness in powder-bed additive manufacturing. Surf Topogr Metrol Prop 2015;3:014003. https://doi.org/10.1088/2051-672X/3/1/014003.
[40] Metelkova J, Ordnung D, Kinds Y, Witvrouw, Van Hooreweder B. Improving the quality of up-facing inclined surfaces in laser powder bed fusion of metals using a dual laser setup. Procedia CIRP 2020;94:266–9. https://doi.org/10.1016/j.procir.2020.09.050.
[41] Nagalingam AP, Vohra MS, Kapur P, Yeo SH. Effect of cut-off, evaluation length, and measurement area in profile and areal surface texture characterization of as-built metal additive manufactured components. Appl Sci 2021;11(11):5089. https://doi.org/10.3390/app11115089.
[42] Thompson A, Senin N, Maskery I, Körner L, Lawes S, Leach R. Internal surface measurement of metal powder bed fusion parts. Addit Manuf 2018;20:126–33. https://doi.org/10.1016/j.addma.2018.01.003.
[43] Jahan S, Wu T, Shin Y, Tovar A, El-Mounayri H. Thermo-fluid topology optimization and experimental study of conformal cooling channels for 3D printed plastic injection molds. Procedia Manuf 2019;34:631–9. https://doi.org/10.1016/j.promfg.2019.06.120.
[44] Ahn DG, Park SH, Kim HS. Manufacture of an injection mould with rapid and uniform cooling characteristics for the fan parts using a DMT process. Int J Precis Eng Manuf 2010;11:915–24. https://doi.org/10.1007/s12541- 010- 0111-3.
[45] Williams RE, Walczyk DF, Dang HT. Using abrasive flow machining to seal and finish conformal channels in laminated tooling. Rapid Prototyp J 2007;13:64–75. https://doi.org/10.1108/13552540710736740.
[46] Wang X, Li S, Fu Y, Gao H. Finishing of additively manufactured metal parts by abrasive flow machining. In: Proc. 27th annu. Int. Solid free. Fabr. Symp; 2016. p. 2470–2.
[47] Gebhardt A. Understanding additive manufacturing - rapid prototyping - rapid tooling - rapid manufacturing. first ed. München: Carl Hanser; 2011.
[48] Dang X-P, Park H-S. Design of U-shape milled groove conformal cooling channels for plastic injection mold. Int J Precis Eng Manuf 2011;12:73–84. https://doi.org/10.1007/s12541-011-0009-8.
[49] Sachs E, Allen S, Guo H, Banos J, Cima M, Serdy J, et al. Progress on Tooling by 3D printing; conformal cooling, dimensional control, surface finish and hardness. In: Solid freeform fabrication proceedings; September 1997. p. 115–23.
[50] Saifullah ABM, Masood SH. Cycle time reduction in injection moulding with conformal cooling channels. In: Proceedings of the international conference on mechanical engineering (ICME 2007), dhaka, Bangladesh, 29–31; December 2007. p. 29–31.
[51] Sun S-H, Ishimoto T, Hagihara K, Tsutsumi Y, Hanawa T, Nakano T. Excellent mechanical and corrosion properties of austenitic stainless steel with a unique crystallographic lamellar microstructure via selective laser melting. Scripta Mater 2019;159:89–93. https://doi.org/10.1016/j.scriptamat.2018.09.017.
[52] Suryawanshi J, Baskaran T, Prakash O, Arya SB, Ramamurty U. On the corrosion resistance of some selective laser melted alloys. Materialia 2018;3:153–61. https://doi.org/10.1016/j.mtla.2018.08.022.
[53] Sander G, Thomas S, Cruz V, Jurg M, Birbilis N, Gao X, et al. On the corrosion and metastable pitting characteristics of 316L stainless steel produced by selective laser melting. J Electrochem Soc 2017;164:C250–7. https://doi.org/10.1149/2.0551706jes.
[54] Samei J, Asgari H, Pelligra C, Sanjari M, Salavati S, Shahriari A, et al. A hybrid additively manufactured martensitic-maraging stainless steel with superior strength and corrosion resistance for plastic injection molding dies. Addit Manuf 2021;45:102068. https://doi.org/10.1016/j.addma.2021.102068.
[55] Bajaj P, Hariharan A, Kini A, Kürnsteiner P, Raabe D, Jägle EA. Steels in additive manufacturing: a review of their microstructure and properties. Mater Sci Eng, A 2020;772:138633. https://doi.org/10.1016/j.msea.2019.138633.
[56] Razavi SMJ, Bordonaro GG, Ferro P, Torgersen J, Berto F. Fatigue behavior of porous Ti-6Al-4V made by laser-engineered net shaping. Materials 2018;11:284. https://doi.org/10.3390/ma11020284.
[57] Combrinck J, Van As B, Booysen GJ, De Beer DJ. Cost-effectiveness of direct metal laser sintered maraging steel inserts for plastic injection moulding process. S Afr J Ind Eng 2019;30:3. https://doi.org/10.7166/30-3-2263.
[58] Minguella-Canela J, Morales Planas S, Gomà Ayats JR, De los Santos López MA. Study and comparison of the different costs' schema associated to geometry, material and processing between 3D printing, injection molding and machining manufacturing technologies. Procedia Manuf 2019;41:280–7. https://doi.org/10.1016/j.promfg.2019.09.010.
[59] Chao-Chyun A, Ren-Haw C. The experimental study on the defects occurrence of SL mold in injection molding. J Mater Process Technol 2008;201(1–3):706–9. https://doi.org/10.1016/j.jmatprotec.2007.11.179.
[60] Xie J, Zhao P, Zhang C, Fu J, Turng L-S. Current state of magnetic levitation and its applications in polymers: a review Sensors. Actuators: Biol Chem 2021;333:129533. https://doi.org/10.1016/j.snb.2021.129533.
[61] Clavería I, Elduque D, Santolaria J, Pina C, Javierre C, Fernández A. The influence of environmental conditions on the dimensional stability of components injected with PA6 and PA66. Polym Test 2016;50:15–25. https://doi.org/10.1016/j.polymertesting.2015.12.008.
[62] EASTAR Copolyester DN011, Preliminary data SheetEastman chemical company. Issue date: 13-September-2002.
[63] Hölker R, Tekkaya AE. Advancements in the manufacturing of dies for hot aluminum extrusion with conformal cooling channels. Int J Adv Manuf Technol 2016;83:1209–20. https://doi.org/10.1007/s00170-015-7647-4.
[64] Ilyas I, Taylor C, Dalgarno K, Gosden J. Design and manufacture of injection mould tool inserts produced using indirect SLS and machining processes. Rapid Prototyp J 2010;16(6):429–40. https://doi.org/10.1108/13552541011083353.